PERGAMON

Available online at www.sciencedirect.com

SCIENCE DIRECT®

Polyhedron 22 (2003) 941–946

POLYHEDRON

www.elsevier.com/locate/poly

Iron(III) nitrilotriacetate and iron(III) iminodiacetate, their X-ray crystallographic structures and chemical properties

Marc Anton Walters [a,*], Vadim Vapnyar [a], Adam Bolour [a], Chris Incarvito [b], Arnold L. Rheingold [b]

[a] *Department of Chemistry, New York University, New York, NY 10003, USA*
[b] *Department of Chemistry, University of Delaware, Newark, DE 19716, USA*

Received 8 March 2002; accepted 10 December 2002

Abstract

Mononuclear iron(III) nitrilotriacetato dichloride, $[Fe(nta)Cl_2]^{2-}$, and iron(III) bis-iminodiacetato, $[Fe(ida)_2]^-$, complexes were formed in py, from which they were isolated and characterized by X-ray crystallography. The iron–nta complex is the structurally simplest of the reported solid state iron–nta complexes, and is catalytic for the air oxidation of hydrogen sulfide to sulfur.

Keywords: Nitrilotriacetate; Iminodiacetate; Iron; Hydrogen sulfide; Crystal structures

1. Introduction

The mononuclear iron(III) nitrilotriacetato moiety ‘Fe(nta)’ is readily obtainable in aqueous solution where it is employed in situ as an important industrial catalyst and as a reagent for biomedical research. As an industrial catalyst Fe(nta) promotes the air oxidation of hydrogen sulfide to elemental sulfur, which is collected for use in other applications, and is known as recovered sulfur. Two thirds of industrial sulfur is recovered sulfur [1]. A second well-known application of [Fe(nta)] is in the oxidative or reductive cleavage of DNA. Investigation of the latter process is important for the prevention and treatment of iron overload disease, which often results in hepatocellular carcinoma [2–5].

We report here the isolation of a low molecular weight mononuclear iron–nta dichloride complex that is catalytic for hydrogen sulfide oxidation and which can serve as a reagent in biological investigations that make use of Fe(nta). The complex has the formula $(pyH)_2[Fe(nta)Cl_2]\cdot H_2O$ (**1**), where py denotes pyridine (Fig. 1). The complex was isolated in high yield from the polar organic solvent py and has been structurally characterized by X-ray crystallography.

The iminodiacetate ligand, ida^{2-}, is related to nta^{3-} because of its similar acid–base properties and metal coordination characteristics. For comparison we explored the synthesis of the iron(III) iminodiacetato moiety, ‘Fe(ida)’, in py and report below on the formation and structural characterization of the resulting complex $(pyH)[Fe(ida)_2]$ (**2**).

2. Experimental

2.1. Synthesis of $(pyH)_2[Fe(nta)Cl_2]\cdot H_2O$ (1)

Nitrilotriacetic acid, $ntaH_3$, (3.54 g, 18.0 mmol) was dissolved in refluxing py (30 ml) which was allowed to cool, resulting in the formation of a flocculent white intermediate. Ferric chloride hexahydrate, $FeCl_3\cdot 6H_2O$, (5 g, 18.0 mmol) was added in lump form and slowly dissolved with stirring to give a dark brown solution that evolved in color to a slightly turbid pale yellowish-green over the course of about 1.5 h. The resulting solution was then concentrated to a viscous oil on a rotary evaporator. Acetonitrile (35 ml) was then layered oil, from which yellow–green crystals began to form

---

* Corresponding author. Tel.: +1-212-998-8477.
E-mail address: marc.walters@nyu.edu (M.A. Walters).

0277-5387/03/$ - see front matter © 2003 Elsevier Science Ltd. All rights reserved.
doi:10.1016/S0277-5387(03)00020-2

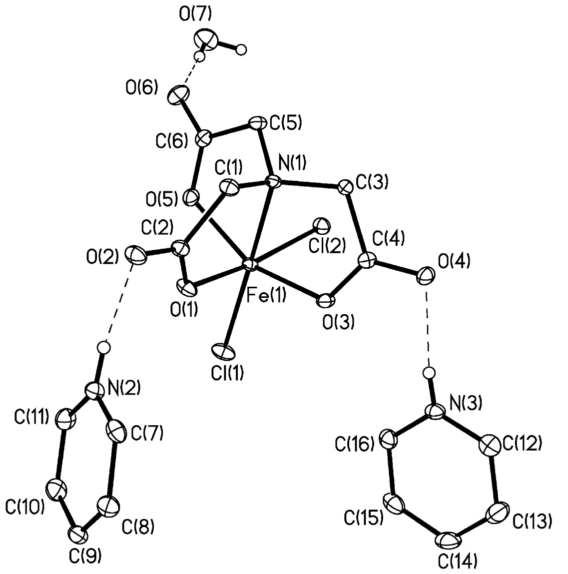

Fig. 1. ORTEP diagram of complex **1**, $[Fe(nta)Cl_2][pyH]_2$. Thermal ellipsoids are drawn at the 40% level. Non-hydrogen bonding hydrogen atoms have been removed for clarity.

after an induction period that ranged from minutes to hours. The solution was allowed to stand overnight to complete the crystallization. The liquid was then decanted and the yellowish-green crystals were washed with CH_3CN (30 ml) and then covered with THF for several hours. Finally the THF was decanted to give 7.56 g of an X-ray diffraction quality crystalline product (83% yield).

Anal. Calc. for $C_{16}H_{20}Cl_2N_3O_7Fe$ (493.115): C, 38.97; H, 4.09; N, 8.52. Found: C, 39.06; H, 3.77; N, 8.47%.

If the initial py solution is allowed to sit overnight, it often deposits a yellow powder that has the composition of complex **1**. *Anal.* Calc. for $C_{16}H_{20}Cl_2N_3O_7Fe$ (493.115): C, 38.97; H, 4.09; N, 8.52. Found: C, 38.89; H, 3.67; N, 8.32%. The powder dissolves readily in water. A saturated aqueous solution of **1** deposits large X-ray diffraction quality crystals (ca. 125 mm^3) when layered with acetonitrile and allowed to stand for several days. Crystals obtained by this method have a unit cell identical to those obtained from py solution.

2.2. Synthesis of $(pyH)[Fe(ida)_2]$ (2)

Iminodiacetic acid, $idaH_2$ (0.50 g, 3.76 mmol) was added to 4 ml of py. After 30 min of stirring, $FeCl_3 \cdot 6H_2O$ (1.02 g, 3.76 mmol) was added giving a dark brown solution. An additional 72 h of stirring resulted in a turbid yellow solution that was centrifuged to remove a yellow precipitate. Acetonitrile, 15 ml, was layered on the yellow supernatant py solution. Crystallization occurred over the course of 3 weeks, to give small yellow crystals interspersed with a microcrystalline orange solid.

2.3. H_2S oxidation

The catalytic oxidation of H_2S was carried out under an H_2S/O_2 atmosphere. A 1 l flask was charged with H_2S, 378.5 Torr (2.1×10^{-2} mole), and O_2, 378.5 Torr (2.1×10^{-2} mol), which constitutes a twofold excess of oxygen. Following this 10 ml of a 52 mM solution of complex **1** (5.2×10^{-4} mol) was added by syringe by injection through the septum cap of the flask. The initially yellow solution became red on contact with the H_2S gas. The solution was stirred for 24 h during which time a precipitate formed. The precipitate was collected by filtration, washed with water, and dried in air.

2.4. X-ray crystallographic data

The solid product had a melting point of 113.5–120°C which was consistent with sulfur. Yield 93%. Data were collected with a Bruker P4/CCD diffractometer. All nonhydrogen atoms were refined with anisotropic thermal parameters and hydrogen atoms were treated as idealized contributions (Table 1).

3. Results and discussion

Reactions between hexaaquoferrate(III) and nta^{3-} in water have been previously explored and have yielded the bis-nta monomer $[Fe(nta)_2]^{3-}$ and the dinuclear complexes $[\{Fe(nta)(H_2O)\}_2(\mu\text{-}O)]^{2-}$ and $[\{Fe(nta)\}_2(\mu\text{-}O)(\mu\text{-}CO_3)]^{4-}$ whose structures have been determined by X-ray crystallography [6–9]. The complex $[Fe(nta)(H_2O)_2]$ formed by reaction between Fe^{3+}(aq) and the acid $ntaH_3$ or the conjugate base nta^{3-} has never been reported. Syntheses aimed at the acquisition of this product have instead yielded insoluble powders, that are plausibly composed of polymers or oligomeric compounds approximated by the chemical formula $[Fe(nta)(H_2O)_2]_n$ [9]. By contrast, complex **1** is unique among simple iron–nta complexes in that it is mononuclear, and like the active catalyst incorporates only a single exogenous ligand, nta^{3-}. Reactions between hexaaquoferrate(III) and ida^{2-} and structural characterizations have likewise been reported earlier [10–14]. The isolation of complex **2**, which has been obtained in other solvents underscores the limits of solvent influence on coordination complex formation.

3.1. Syntheses

In the synthesis of **1** we eschewed standard synthetic routes in aqueous solution that have afforded isolable dinuclear complexes containing μ-oxo bridged Fe(nta) groups [8,9]. Instead, syntheses were carried out in py, which serves as a solvent, a base for the deprotonation of $ntaH_3$, and ultimately provides a pyridinium (pyH^+)

Table 1
Crystallographic structural determinations

Empirical formula	$C_{16}H_{20}Cl_2FeN_3O_7$ (**1**)	$C_{13}H_{16}FeN_3O_8$ (**2**)
Formula weight	493.13	398.14
Temperature (K)	173(2)	100(2)
Wavelength (Å)	0.71073	0.71073
Crystal system	monoclinic	monoclinic
Space group	$P2_1/n$	$C2/c$
Unit cell dimensions		
a (Å)	12.2471(7)	15.692(2)
b (Å)	13.0154(8)	5.4815(7)
c (Å)	12.7530(7)	18.317(2)
β (°)	97.3970(10)	99.882(4)
Volume (Å^3)	2015.9(2)	1552.2(4)
Z	4	4
Density (calculated) (g cm^{-3})	1.625	1.704
Absorption coefficient (mm^{-1})	1.057	1.023
$F(000)$	1012	820
Crystal size (mm)	0.30 × 0.30 × 0.28	0.25 × 0.25 × 0.25
θ Range for data collection (°)	2.25–28.33	2.26–28.29
Index ranges	$-15 \leq h \leq 14$, $-15 \leq k \leq 11$, $-17 \leq l \leq 16$	$-20 \leq h \leq 20$, $-7 \leq k \leq 7$, $-24 \leq l \leq 23$
Reflections collected	9466	8532
Independent reflections	4329 [$R_{int} = 0.0247$]	1869 [$R_{int} = 0.0198$]
Completeness to θ	28.33°, 86.2%	28.29°, 96.9%
Absorption correction	empirical from SADABS	empirical from SADABS
Refinement method	full-matrix least-squares on F^2	full-matrix least-squares on F^2
Data/restraints/parameters	4329/0/278	1869/0/120
Goodness-of-fit on F^2	1.099	1.096
Final R indices [$I > 2\sigma(I)$] [a,b]	$R_1 = 0.0356$, $wR_2 = 0.0789$	$R_1 = 0.0459$, $wR_2 = 0.1225$
R indices (all data)	$R_1 = 0.0432$, $wR_2 = 0.0817$	$R_1 = 0.0464$, $wR_2 = 0.1227$
Largest difference peak and hole (e Å^{-3})	0.391 and −0.398	0.472 and −0.373

[a] $R = \Sigma||F_o| - |F_c||/\Sigma|F_o|$.

[b] $R(wF^2) = \{\Sigma[w(F_o^2 - F_c^2)^2]/\Sigma[w(F_o^2)^2]\}^{1/2}$; $w = 1/[s^2(F_o^2) + (aP)^2 + bP]$, $P = [2F_c^2 + \max(F_o,0)]/3$.

counterion. The py solvent may also serve to displace water from the starting complex $FeCl_3 \cdot 6H_2O$ and thus favor the formation of complex **1**, which is unusual among simple iron–nta complexes because of the absence of water, hydroxide ion, or an oxo group in its coordination sphere. Crystals of **1** are obtained directly from py by the addition of CH_3CN and exhibit long term stability in the solid state. As described in the Section 2 complex **1** is freely soluble in water and alcohols and is obtainable either as macroscopic single crystals or as a free flowing yellow powder. Crystals of **1** from water have the same unit cell as those of complexes that are isolated from py.

A similar synthetic approach was employed in the synthesis of complex **2**. Complex **2** was obtained from a 1:1 Fe:idaH_2 solution in py. Only the yellow bis-ida iron complex $[Fe(ida)_2]^-$ was isolated. The product was co-deposited with an orange powder. While the product was unsuited for elemental analysis, handpicked crystals yielded to single crystal X-ray crystallography. The unit cells of several crystals examined in the sample identified as **2** were identical.

3.2. Crystal structure of $(pyH)_2[Fe(nta)Cl_2] \cdot H_2O$

Complex **1** has a distorted octahedral structure with approximate C_s point group symmetry. The nitrogen atom, which is relatively weakly bound, is far from iron, with a Fe–N bond length of 2.2355(16) Å. By contrast the carboxylate oxygen atoms have an average Fe–O bond length of 2.00 Å. The Fe–Cl bond lengths which average 2.31 Å, are typical of Fe(III)–Cl distances [15,16]. The $[Fe^{3+}(nta)]$ coordination geometry and dimensions closely resemble those of other $[Fe^{3+}(nta)]$ complexes [8,9,17]. One pyridinium counterion is hydrogen bonded to a carboxylate oxygen on each of two arms of nta. A water molecule is hydrogen bonded to a carboxylate oxygen on a third arm of the ligand. The respective N–H···O and O–H···O donor–acceptor distances are 2.675(3) and 2.718(2) Å for the pyridinium donors and 2.792(3) Å for the water donor. There is no obvious effect of N–H···O or O–H···O hydrogen bonding on the bond lengths or geometry of complex **1** (Table 2).

3.3. Crystal structure of $(pyH)[Fe(ida)_2] \cdot H_2O$

The iron in complex **2** is six coordinate and the complex has distorted C_2 point group symmetry. Both the Fe complex and the pyH^+ counterion reside on crystallographic twofold axes. Only half of each is present in the asymmetric unit. We refined only three positions of pyH^+ and, therefore, treated one of the positions as a mixture of nitrogen and carbon (NC) (Fig. 2). The ida ligands are facially coordinated with the weakly bound nitrogen atoms *trans* to a carboxylate oxygen of the opposing ligand. The Fe–N bond length is 2.161(3) Å. The average carboxylate–iron distance is 1.982(2) Å. The complex anion is isostructural with another complex $[Fe(ida)_2]^-$ that has been mentioned in review but for which crystallographic data has not been reported [10,18]. The pyridinium cation and the imino group both serve as hydrogen bond donors. A bifurcated hydrogen bond links pyridinium to carboxylate oxygens O(3) and O(4). The corresponding N–O distances are 3.21(1) and 3.01(1) Å, respectively. Similarly, the N–H group of the ida ligand forms hydrogen bonds of length 2.96(1) and 3.11(1) Å with the carboxylate oxygens O(1) and O(2), respectively, on an adjacent complex (Table 3).

Table 2
Bond lengths (Å) and angles (°) for $(pyH)_2[Fe(nta)Cl_2]\cdot H_2O$ (**1**)

Bond lengths	
Fe(1)–O(5)	1.9783(15)
Fe(1)–O(3)	2.0223(14)
Fe(1)–O(1)	2.0245(17)
Fe(1)–N(1)	2.2355(16)
Fe(1)–Cl(1)	2.2732(6)
Fe(1)–Cl(2)	2.3565(7)
O(1)–C(2)	1.269(2)
O(2)–C(2)	1.236(3)
O(3)–C(4)	1.272(2)
O(4)–C(4)	1.244(3)
O(5)–C(6)	1.285(3)
O(6)–C(6)	1.228(3)
N(1)–C(1)	1.471(3)
N(1)–C(3)	1.471(3)
N(1)–C(5)	1.479(3)
N(2)–C(7)	1.331(3)
N(2)–C(11)	1.340(3)
N(3)–C(12)	1.329(3)
N(3)–C(16)	1.339(3)
C(1)–C(2)	1.522(3)
C(3)–C(4)	1.516(3)
C(5)–C(6)	1.522(3)
C(7)–C(8)	1.371(3)
C(8)–C(9)	1.385(3)
C(9)–C(10)	1.371(3)
C(10)–C(11)	1.374(3)
C(12)–C(13)	1.377(3)
C(13)–C(14)	1.379(4)
C(14)–C(15)	1.375(4)
C(15)–C(16)	1.367(3)
O(7)–H(7A)···O(6)	2.792(3) [a]
N(2)–H(2)···O(2)	2.675(3)
N(3)–H(3C)···O(4)	2.718(2)
Bond angles	
O(5)–Fe(1)–O(3)	153.96(6)
O(5)–Fe(1)–O(1)	89.52(7)
O(3)–Fe(1)–O(1)	89.11(7)
O(5)–Fe(1)–N(1)	77.53(6)
O(3)–Fe(1)–N(1)	76.61(6)
O(1)–Fe(1)–N(1)	80.26(6)
O(5)–Fe(1)–Cl(1)	106.73(5)
O(3)–Fe(1)–Cl(1)	99.30(4)
O(1)–Fe(1)–Cl(1)	91.44(4)
N(1)–Fe(1)–Cl(1)	170.73(5)
O(5)–Fe(1)–Cl(2)	88.13(5)
O(3)–Fe(1)–Cl(2)	89.35(5)
O(1)–Fe(1)–Cl(2)	171.35(4)
N(1)–Fe(1)–Cl(2)	91.10(5)
Cl(1)–Fe(1)–Cl(2)	97.21(2)
C(2)–O(1)–Fe(1)	119.21(14)
C(4)–O(3)–Fe(1)	118.41(13)
C(6)–O(5)–Fe(1)	119.76(13)
C(1)–N(1)–C(3)	113.05(16)
C(1)–N(1)–C(5)	112.43(17)
C(3)–N(1)–C(5)	113.03(17)
C(1)–N(1)–Fe(1)	107.16(12)
C(3)–N(1)–Fe(1)	105.95(12)
C(5)–N(1)–Fe(1)	104.42(11)
C(7)–N(2)–C(11)	122.2(2)
C(12)–N(3)–C(16)	123.0(2)
N(1)–C(1)–C(2)	114.69(16)
O(2)–C(2)–O(1)	124.7(2)
O(2)–C(2)–C(1)	116.94(18)
O(1)–C(2)–C(1)	118.4(2)
N(1)–C(3)–C(4)	110.65(16)
O(4)–C(4)–O(3)	123.75(19)
O(4)–C(4)–C(3)	118.81(18)
O(3)–C(4)–C(3)	117.42(18)
N(1)–C(5)–C(6)	111.06(16)
O(6)–C(6)–O(5)	124.8(2)
O(6)–C(6)–C(5)	119.33(19)
O(5)–C(6)–C(5)	115.88(17)
N(2)–C(7)–C(8)	120.0(2)
C(7)–C(8)–C(9)	119.1(2)
C(10)–C(9)–C(8)	119.5(2)
C(9)–C(10)–C(11)	119.5(2)
N(2)–C(11)–C(10)	119.5(2)
N(3)–C(12)–C(13)	119.2(2)
C(12)–C(13)–C(14)	119.0(2)
C(15)–C(14)–C(13)	120.3(2)
C(16)–C(15)–C(14)	118.8(2)
N(3)–C(16)–C(15)	119.7(2)

[a] Hydrogen bond distance in the D–H···A interaction is for the D···A separation.

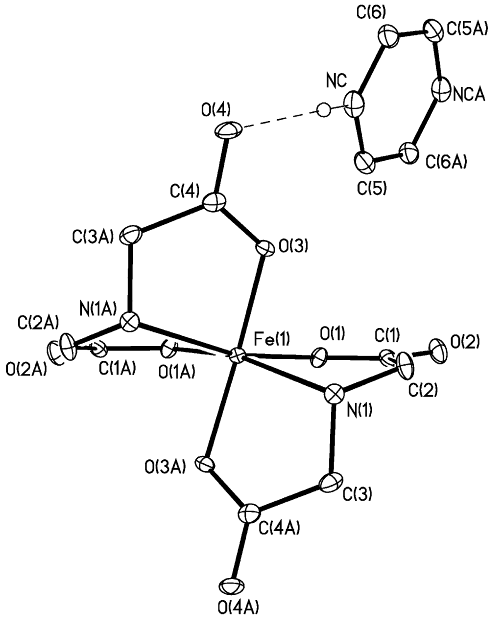

Fig. 2. ORTEP diagram of complex **2**, $[Fe(ida)_2][pyH]$. Thermal ellipsoids are drawn at the 40% level. Non-hydrogen bonding hydrogen atoms have been removed for clarity.

3.4. *^{1}H-NMR spectra*

The proton NMR spectrum of $ntaH_3$ in DMSO-d_6 has a single methylene proton peak at 3.6 ppm. As expected for complex **1**, which is paramagnetic, the ligand proton resonances are shifted by dipolar interactions with the metal ion. Peaks for **1** appeared at 11.3 (0.94H, pyH^+), 10.7 (0.55H, pyH^+), 10.25 (0.94H, pyH^+), 5.95 (10.6H, pyH^+), and 5.00 ppm (6H, nta^{3-}). The py resonances were assigned in part on the basis of their integrated intensities. The positions of the pyH^+ resonances are consistent with iron(III)–

Table 3
Bond lengths (Å) and angles (°) for (pyH)[Fe(ida)$_2$] (**2**)

Bond lengths	
Fe(1)–O(1)	1.980(2)
Fe(1)–O(3)	1.984(2)
Fe(1)–N(1)	2.161(3)
O(1)–C(1)	1.303(4)
O(2)–C(1)	1.219(4)
O(3)–C(4)	1.283(4)
O(4)–C(4)	1.238(4)
N(1)–H(1)	0.81(5)
N(1)–C(3)	1.473(4)
N(1)–C(2)	1.477(4)
C(1)–C(2)	1.519(5)
C(3)–C(4)#1	1.505(5)
C(5)–C(6)#2	1.373(6)
C(5)–NC	1.375(6)
C(6)–NC	1.368(5)
N(1)–H(1)···O(1)#3	2.96(1)
N(1)–H(1)···O(2)#3	3.11(1)
NC–HCA···O(3)#1	3.21(1)
NC–HCA···O(4)#1	3.01(1)
Bond angles	
O(1)#1–Fe(1)–O(1)	88.25(14)
O(1)#1–Fe(1)–O(3)#1	91.97(10)
O(1)–Fe(1)–O(3)#1	108.58(10)
O(1)–Fe(1)–O(3)	91.97(10)
O(3)#1–Fe(1)–O(3)	151.54(16)
O(1)#1–Fe(1)–N(1)#1	79.81(10)
O(1)–Fe(1)–N(1)#1	161.87(10)
O(3)#1–Fe(1)–N(1)#1	85.60(10)
O(3)–Fe(1)–N(1)#1	79.16(10)
O(1)#1–Fe(1)–N(1)	161.87(10)
O(1)–Fe(1)–N(1)	79.81(10)
O(3)#1–Fe(1)–N(1)	79.16(10)
O(3)–Fe(1)–N(1)	85.60(10)
N(1)#1–Fe(1)–N(1)	114.80(16)
C(1)–O(1)–Fe(1)	118.8(2)
C(4)–O(3)–Fe(1)	120.9(2)
H(1)–N(1)–C(3)	110(3)
H(1)–N(1)–C(2)	109(3)
C(3)–N(1)–C(2)	114.0(3)
H(1)–N(1)–Fe(1)	107(3)
C(3)–N(1)–Fe(1)	109.6(2)
C(2)–N(1)–Fe(1)	106.4(2)
O(2)–C(1)–O(1)	123.9(3)
O(2)–C(1)–C(2)	120.4(3)
O(1)–C(1)–C(2)	115.6(3)
N(1)–C(2)–C(1)	111.7(3)
N(1)–C(3)–C(4)#1	111.6(3)
O(4)–C(4)–O(3)	123.7(3)
O(4)–C(4)–C(3)#1	119.7(3)
O(3)–C(4)–C(3)#1	116.5(3)
C(6)#2–C(5)–NC	120.1(3)
NC–C(6)–C(5)#2	119.5(4)
C(6)–NC–C(5)	120.4(4)

Symmetry transformations used to generate equivalent atoms: #1 $-x+2, y, -z+3/2$; #2 $-x+3/2, -y-1/2, -z+1$; #3 $x, y+1, z$.

pyH$^+$ dipolar coupling, perhaps accompanied by an exchange processes involving the H-bonding association and dissociation of pyH$^+$ and the Fe complex [19]. An alternative but less likely view is that the exchange is between py and Cl$^-$ as ligating groups. However, covalent bonding between py and high-spin ferric iron gives contact-shifted resonances in the range of 20–120 ppm, which are not observed for complex **1** [20,21].

3.5. H_2S oxidation

Current sulfur recovery processes employ chelated iron(III) as a hydrogen sulfide oxidant. A catalyst of particular importance for this process, iron nitrilotriacetate, is reportedly formed only in situ through the reaction of $Fe(NO_3)_3 \cdot 9H_2O$ with nitrilotriacetic acid (ntaH$_3$) in 1:1 ratio to form an Fe(nta) (aq) complex in basic solution [22]. We have found that only $FeCl_3 \cdot 6H_2O$ reacts with ntaH$_3$ in py to yield an isolable complex in pure form. The $Fe(NO_3)_3 \cdot 9H_2O$ reacts to give a polycrystalline mixture that has not yet been characterized. When formed from $Fe(NO_3)_3 \cdot 9H_2O$ and ntaH$_3$ in water, the Fe(nta) catalyst for H_2S oxidation must be structurally different from complex **1**. Complex **1**, however, is an effective catalyst for the oxidation of H_2S by the reaction:

$$H_2S + \frac{1}{2}\ O_2 \rightarrow H_2O + \frac{1}{8}\ S_8$$

Preliminary experiments gave pure sulfur in 93% yield (47 turnovers) from H_2S in a closed reactor.

In summary, the reaction between $FeCl_3 \cdot 6H_2O$ and ntaH$_3$ or idaH$_2$ in py results in the formation of mononuclear complexes **1** and **2**. Complex **1** is isolated as a crystalline complex that is freely soluble in water and catalyzes the oxidation of H_2S to S. Further it exhibits long term stability in the solid state and provides a ready form of a catalytic reagent for industrial or laboratory applications.

Acknowledgements

This investigation was supported by a New York University Research Challenge Fund grant to M.A.W.

References

[1] M. Capone, in: M. Howe-Grant (Ed.), Sulfur Removal and Recovery, vol. 23, 4th Ed., Wiley, NewYork, 1991, p. 432.
[2] S. Toyokuni, J.-L. Sagripanti, Free Radic. Res. 31 (1999) 123.
[3] V. Abalea, J. Cillard, M.-P. Dubos, J.-P. Anger, P. Cillard, I. Morell, Carcinogenesis 19 (1998) 1053.
[4] A. Asaumi, T. Ogino, T. Akiyama, T. Kawabata, S. Okada, Biochem. Mol. Biol. Int. 39 (1996) 77.
[5] S. Toyokuni, J.-L. Sagripanti, Carcinogenesis (London) 14 (1993) 223.
[6] M. Krishnamurthy, K.B. Morris, J. Inorg. Nucl. Chem. 34 (1972) 719.

[7] W. Clegg, A.K. Powell, M.J. Ware, Acta Crystallogr., Sect. C 40 (1984) 1822.

[8] T. Fujita, S. Ohba, Y. Nishida, A. Goto, T. Kokii, Acta Crystallogr., Sect. C: Cryst. Struct. Commun. C50 (1994) 544.

[9] S.L. Heath, A.K. Powell, H.L. Utting, M. Helliwell, J. Chem. Soc., Dalton Trans. (1992) 305.

[10] A. Mandel, W. Schmitt, T.G. Womack, R. Bhalla, R.K. Henderson, S.L. Heath, A.K. Powell, Coord. Chem. Rev. 190–192 (1999) 1067.

[11] J. Wang, W. Zhang, X. Song, X. Zhang, Y. Xing, Y. Lin, H. Jia, L. Zhang, Wuji Huaxue Xuebao 14 (1998) 96.

[12] J. Wang, W.Q. Zhang, X.M. Song, X.D. Zhang, Y. Xing, Y.H. Lin, H.Q. Jia, L. Zhang, Chin. Chem. Lett. 8 (1997) 741.

[13] Y.-G. Wei, S.-W. Zhang, M.-C. Shao, Polyhedron 16 (1997) 2307.

[14] C.J. Harding, R.K. Henderson, A.K. Powell, Angew. Chem. 105 (1993) 583.

[15] J.A. Bertrand, E. Fujita, P.G. Eller, D.G. VanDerveer, Inorg. Chem. 17 (1978) 3571.

[16] T.B. Murphy, N.J. Rose, V. Schomaker, A. Aruffo, Inorg. Chim. Acta 108 (1985) 183.

[17] L.S. White, P.V. Nilsson, L.H. Pignolet, L. Que, Jr., J. Am. Chem. Soc. 106 (1984) 8312.

[18] R.K. Henderson, Ph.D. thesis, University of East Anglia, Norwich, UK, 1993.

[19] G.N. La Mar, in: G.N. La Mar, W.D. Horrocks, Jr., R.H. Holm (Eds.), Novel Structural Studies in Solution, Academic Press, New York, 1973, p. 387.

[20] A.P. Sobolev, D.E. Babushkin, A.A. Shubin, E.P. Talsi, J. Molec. Catal. A: Chem. 112 (1996) 253.

[21] I. Vernik, D.V. Stynes, Inorg. Chem. 35 (1996) 2011.

[22] D. McManus, A.E. Martell, J. Mol. Catal. A: Chem. 117 (1997) 289.